Relationship between and effect of inelastic excitations and transfer channels on sub-barrier fusion enhancement

Khushboo,[1,*] S. Mandal,[1] S. Nath,[2] N. Madhavan,[2] J. Gehlot,[2] A. Jhingan,[2] Neeraj Kumar,[1] Tathagata Banerjee,[2] Gurpreet Kaur,[3] K. Rojeeta Devi,[1] A. Banerjee,[1] Neelam,[1] T. Varughese,[2] Davinder Siwal,[1,3] R. Garg,[1,2] Ish Mukul,[2] M. Saxena,[1] S. Verma,[1] S. Kumar,[1] B. R. Behera,[3] and P. Verma[4]

[1]*Department of Physics and Astrophysics, University of Delhi, Delhi 110007, India*

[2]*Inter University Accelerator Centre, Aruna Asaf Ali Marg, New Delhi 110067, India*

[3]*Department of Physics, Panjab University, Chandigarh 160014, India*

[4]*Department of Physics, Kalindi College, University of Delhi, Delhi 110008, India*

(Received 17 November 2016; revised manuscript received 5 April 2017; published 21 July 2017)

Background: It is a well established fact that nuclear deformation and vibration influence fusion dynamics around the Coulomb barrier. This effect was observed for several systems with the inclusion of inelastic excitations in coupled-channels calculations. Sub-barrier fusion cross sections were also observed to be affected by neutron transfer in systems carrying positive Q value for transfer channels. However, recent experimental analysis with a few systems showed that inelastic excitations are enough to explain the sub-barrier fusion behavior, and no effect was noticed due to positive Q-value transfer channels.

Purpose: The motivation behind present investigation is to explore the effects of colliding nuclei structure and the transfer channel on enhancement of sub-barrier fusion cross sections.

Method: An experiment was performed with Heavy Ion Reaction Analyzer (HIRA) at New Delhi to measure the fusion cross sections for ^{28}Si + ^{92,96}Zr systems. These cross sections were later compared with quantum mechanical coupled-channels calculations. In order to explore the effects of nuclear deformation on fusion cross sections, the present data were compared with those of other researchers on fusion who have used various projectiles of different structural properties on a ^{96}Zr target.

Results: Experimental fusion cross sections have been extracted around the Coulomb barrier. In the coupled-channels framework, inclusion of inelastic excitations of both projectile (^{28}Si) and targets (^{92,96}Zr) could reproduce the experimental cross sections around the Coulomb barrier, but they deviated substantially in the sub-barrier region. This indicates that positive Q-value neutron transfer channels may need to be included in the calculations to reproduce the experimental cross sections at sub-barrier energies.

Conclusions: The nuclear structure of interacting nuclei has a strong influence on sub-barrier fusion enhancement. The effect of multineutron transfer channels was observed to be significant for fusion, especially for those systems where interacting nuclei are less deformed or spherical.

DOI: 10.1103/PhysRevC.96.014614

I. INTRODUCTION

The mechanism involved in enhancement of sub-barrier fusion cross sections is one of the topics of recent research. In the vicinity of the Coulomb barrier, various intrinsic degrees of freedom influence fusion dynamics, which include nuclear deformation, surface vibrations and nucleon transfer. The coupling of these degrees of freedom is responsible for sub-barrier fusion enhancement. Nuclear deformation and surface vibrations split the single barrier of interacting nuclei according to their rotation and shape variation, which enhance fusion cross sections at low energies [1]. Past experimental and theoretical investigations on barrier distributions have confirmed the role of nuclear static deformation [2,3] and surface vibrations [4–7] on fusion processes. Neutrons which are unaffected by the Coulomb barrier can transfer even at large distances, increasing fusion probability between colliding nuclei [8,9].

Enhancement in sub-barrier fusion cross sections due to nuclear deformation has been demonstrated in the existing literature with different isotopes of samarium [10], where the shape of the isotopes (^{148,150,152,154}Sm) varied from spherical to deformed. A significant increase in sub-barrier fusion cross sections was clearly observed for Sm isotopes with larger deformation. A similar effect due to static deformation has also been explored for ^{40}Ca + ^{192}Os,^{194}Pt systems within the framework of coupled-channels (CC) calculations [11]. The nuclei ^{192}Os and ^{194}Pt have similar quadrupole deformation strengths, but exhibit different shapes: ^{192}Os ($\beta_2 = 0.167$) is prolate deformed whereas ^{194}Pt ($\beta_2 = -0.154$) is an oblate deformed nucleus. The effect of nuclear shape on fusion cross sections was also indicated in the article. In an experiment performed with a pair of systems, ^{36}S + ^{90,96}Zr, fusion cross sections were found to be relatively larger for ^{96}Zr than ^{90}Zr [12]. These cross sections have been analyzed with theoretical CC calculations, and enhancement observed in ^{96}Zr has been attributed to the strong octupole vibration of ^{96}Zr. Later, a similar kind of behavior was also exhibited by a ^{48}Ca projectile on ^{90,96}Zr targets [13]. Moreover, multiphonon coupling has been observed to be important for ^{96}Zr. The effect of multi

*s12khushboo@gmail.com

phonon couplings was also illustrated with a few systems by Esbensen [14]. Here, it was mentioned that multiphonon states become extremely important for soft and heavy nuclei. A pure experimental comparison was presented with several Ca + Zr systems [15] in an adjusted energy scale, where a remarkable enhancement in fusion cross sections was observed for ^{94,96}Zr. For both these nuclei, neutron transfer might be responsible for the large enhancement, as low-lying vibrational excitations could not explain the fusion cross sections at low energies.

Large enhancement in fusion yield due to neutron transfer channels has been observed in systems carrying positive Q value for transfer channels, and was first noticed in Ni + Ni systems [16,17]. Later, similar behavior was observed in a variety of medium mass systems such as ^{28}Si + ^{94}Zr [18], ^{32}S + ^{48}Ca [19], ^{40}Ca + ^{48}Ca [20,21], and ^{32}S + ^{96}Zr [22]. However, there is strong evidence only where inelastic excitations are enough to explain the sub-barrier cross sections. Despite the positive Q value for neutron transfer channels, ^{60}Ni + ^{100}Mo did not show any significant enhancement [23]. Reduced fusion cross sections show almost the same behavior for ^{132}Sn + ^{58}Ni and ^{64}Ni + ^{118}Sn, where Q values for the systems are extremely different [24]. Similar fusion behavior has also been exhibited by ^{16}O + ^{76}Ge and ^{18}O + ^{74}Ge systems [25]. It has been argued that the neutron transfer weakly affects fusion if the deformation strength of the colliding nuclei do not change or decrease after transfer [26]. This argument has been supported by investigation of other authors [27,28]. Recently, it was observed that only outermost neutrons (mainly one and two neutron transfer channels with $Q > 0$) give a noticeable contribution to fusion even though the Q value is positive for many neutron transfer channels. It has also been emphasized that significant contribution from the transfer channels can be expected if coupling to collective states is less important, i.e. for spherical or magic nuclei [29].

In recent research, fusion cross sections were measured for systems ^{40}Ca + ^{58,64}Ni [30], and a noticeable impact of the projectile as well as target structure was observed on fusion. Apart from this, the importance of neutron transfer for ^{64}Ni was pointed out while reproducing the experimental data of ^{64}Ni by incorporating the Q value corresponding to the first excited 0^+ state of ^{42}Ca. More recently, the effect of nuclear structure was examined through measurement of fusion cross sections with two systems, ^{48}Ti + ^{58}Fe and ^{58}Ni + ^{54}Fe [31]. ^{48}Ti and ^{58}Fe are soft nuclei, whereas ^{58}Ni and ^{54}Fe are rigid. Different trends of fusion excitation function were observed for the two systems in the sub-barrier region, which was related to the different structure of participating nuclei. It was mentioned that strong quadrupole modes of ^{48}Ti and ^{58}Fe might be responsible for the less steep slope observed in fusion excitation function of ^{48}Ti + ^{58}Fe system. The nuclei Ca, Ni, and Ti were also examined recently by Liang *et al.* [32] and importance of both transfer channels and inelastic excitations on sub-barrier fusion was highlighted. Fusion cross sections were measured for systems ^{46,50}Ti + ^{124}Sn and compared with fusion behavior of ^{40}Ca + ^{124}Sn and ^{58}Ni + ^{124}Sn. The comparison indicated the role of transfer coupling on fusion due to the presence of positive Q values in systems ^{40}Ca,^{46}Ti + ^{124}Sn. Along with neutron transfer, a significant effect of octupole state of ^{40}Ca was noticed in the barrier distributions, which was responsible for large sub-barrier fusion enhancement in ^{40}Ca induced reactions.

In spite of extensive research, the role of transfer to sub-barrier fusion is still not understood in detail, and offers an open area to explore the effects of rearrangement of nucleons along with nuclear structure. Inelastic excitations seem to be important in some systems while transfer channel dominates in others for sub-barrier fusion. To examine the role of nuclear structure along with transfer channel Q value, ^{92,96}Zr targets were selected along with an oblate shaped projectile, ^{28}Si, which has large negative β_2 of its lowest 2^+ collective state. Target ^{96}Zr has already been explored with spherical and prolate deformed projectiles [22,33]. The strong octupole state of ^{96}Zr with the presence of six neutrons outside the closed shell and the large deformation strength of ^{28}Si ($\beta_2 = -0.407$) make the ^{28}Si + ^{96}Zr system suitable for the study of nuclear structure as well as transfer channel effects. The target ^{92}Zr has two neutrons outside its closed shell and has positive Q value for only a two-neutron pick-up channel. Hence, the comparison of two isotopes will be helpful in investigating the importance of two-neutron or multineutron transfer on purely experimental basis. The fusion excitation function for ^{28}Si + ^{90,92,94}Zr is already measured [18,34]. Therefore, four Zr isotopes can be used to show experimentally the variation of fusion enhancement with a successive increase of transferring neutrons.

The present paper is arranged as follows: Experimental technique along with relevant details of the experimental setup and detectors used during the experiment are presented in Sec. II. Extracted fusion cross sections along with theoretical description within a coupled-channels formalism are discussed in Sec. III. A comparison is provided for different projectiles with ^{96}Zr target nuclei. A brief summary of the entire work is given in Sec. IV.

II. EXPERIMENTAL DETAILS

The present experiment was performed with the Pelletron accelerator of Inter University Accelerator Centre (IUAC), New Delhi, India. A ^{28}Si pulsed beam of 1 and 2 μs pulse separation with time width of 1 ns was used to bombard $^{96}ZrO_2$ and ^{92}Zr targets. The isotopically enriched ^{96}Zr (86.4%) and ^{92}Zr (95.13%) targets, of thicknesses 85 and 265 μg/cm^2 respectively, were prepared on carbon backings of thicknesses 20 and 50 μg/cm^2 respectively, using the electron beam evaporation technique [35,36]. Fusion cross-section measurements for ^{96}Zr were carried out in steps of 2–4 MeV from beam energies of 81.4 to 119.5 MeV, covering a range from 14% below to 26% above the Coulomb barrier (V_b) [37]. Fusion cross sections for ^{28}Si + ^{92}Zr were measured at a few energies. Some of the cross sections for the system ^{28}Si + ^{92}Zr are taken from literature [34]. The fusion cross sections for ^{28}Si + ^{96}Zr are corrected for isotopic impurity in the target of $^{96}ZrO_2$. Fusion cross sections were measured using the Heavy Ion Reaction Analyzer (HIRA) [38], which was kept at zero degree with respect to beam with solid angle coverage of 5 msr.

Evaporation residues (ERs) arriving at the focal plane of HIRA were detected through a 15.2 × 5.1 cm^2 multiwire proportional counter (MWPC) operated at a pressure of 3 mbar

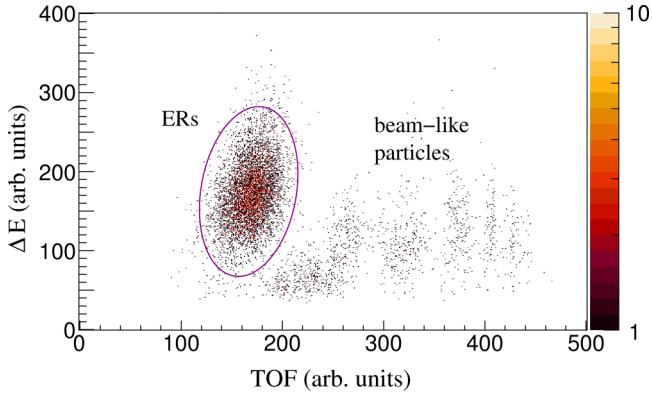

FIG. 1. Two-dimensional spectrum of energy loss (ΔE) vs TOF at $E_{\rm lab} = 111$ MeV for the ^{28}Si + ^{96}Zr system.

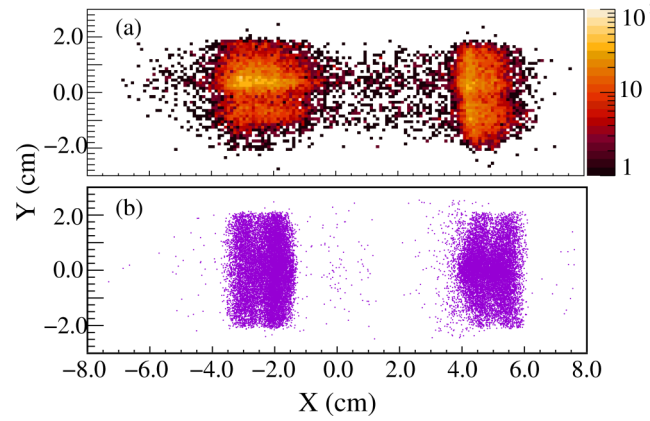

FIG. 2. MWPC position spectrum obtained (a) experimentally and (b) from simulation of the ^{28}Si + ^{96}Zr system at $E_{\rm lab} = 96$ MeV.

of isobutane gas. Inside the target chamber, two silicon-surface barrier detectors (SSBDs) were mounted symmetrically at $\theta_{\rm lab} = 15.5^0$ with respect to beam direction and at a distance of 10 cm from the target. These detectors were used to monitor the beam direction during the online experiment and for normalization of cross sections during data analysis. A carbon foil of thickness 30 μg/cm^2 was placed 10 cm downstream from the target to reset the charge state of ERs after the internal conversion process.

The ERs were selected through the two-dimensional spectrum of ER energy loss (ΔE) vs ER time of flight (TOF) as shown in Fig. 1. Offline data analysis was performed using CANDLE software [39].

III. DATA ANALYSIS AND RESULTS

The fusion cross section for a system is given as the sum of ER and fission cross sections. In the present system, the probability of fission to occur is expected to be insignificant, and hence fusion cross section will be equal to the ER cross section. ER cross sections were extracted using the following formula:

$$\sigma_{\rm fus} = \sigma_{\rm ER} = \left(\frac{Y_{\rm ER}}{Y_{\rm M}}\right)\left(\frac{d\sigma}{d\Omega}\right)_{\rm R}\Omega_{\rm M}\frac{1}{\eta}, \qquad (1)$$

where $Y_{\rm ER}$ is the yield of the ER at the focal plane of HIRA, $Y_{\rm M}$ is the yield of elastic events in the monitor detectors, $(\frac{d\sigma}{d\Omega})_{\rm R}$ is the differential Rutherford cross section at the monitor angle in laboratory frame, $\Omega_{\rm M}$ is the solid angle subtended by the monitor detectors, and η is the transmission efficiency of HIRA for ERs.

The precise ER transmission efficiency through HIRA can be estimated theoretically from the semimicroscopic Monte Carlo code TERS [40]. This code simulates HIRA and gives absolute transmission efficiency for a system. An experimental spectrum was created between x and y positions of the MWPC gated by ERs of the ΔE-TOF spectrum (as shown in Fig. 1 for $E_{\rm lab} = 111$ MeV). A similar position spectrum was generated using TERS code. For comparison, the two-dimensional representation of the MWPC position spectra obtained experimentally (upper panel) and from simulation (lower panel) are shown in Fig. 2, which indicates the agreement between the experimental and simulation results.

Here, two dark square areas correspond to two different A/q (mass/charge state) of evaporation residues. In the present case, average HIRA efficiency was estimated from simulation code TERS for different ERs at all the beam energies. The simulated efficiency was 6.1% for ^{28}Si + ^{96}Zr and 4.0% for ^{28}Si + ^{92}Zr at 96 MeV beam energy. The uncertainty of 10% is expected in the simulated value with respect to the measured efficiency in different systems [18,40].

Fusion cross sections obtained using Eq. (1) are given in Table I. The quoted energies are corrected for energy loss in the carbon backing and target half thickness. The experimental error includes statistical error and the error in HIRA efficiency.

TABLE I. Experimental fusion cross sections at center-of mass-energies for ^{28}Si + ^{96}Zr and ^{28}Si + ^{92}Zr systems.

$E_{\rm c.m.}$ (MeV)	$\sigma_{\rm fus} \pm \Delta\sigma_{\rm fus}$ (mb)
^{28}Si + ^{96}Zr	
63.0	0.11 ± 0.02
64.5	1.43 ± 0.22
66.1	7.03 ± 1.06
67.7	20.23 ± 3.07
69.2	39.19 ± 5.92
70.8	51.76 ± 7.80
72.4	116.3 ± 17.6
73.9	159.8 ± 24.6
75.4	212.7 ± 32.5
77.7	317.4 ± 48.0
80.1	397.6 ± 60.1
83.2	485.4 ± 74.1
85.5	548.8 ± 83.5
89.4	689.8 ± 104.6
92.5	778.6 ± 121.9
^{28}Si + ^{92}Zr	
67.8	7.03 ± 1.06
70.9	53.68 ± 8.06
76.3	253.02 ± 37.98
84.0	535.69 ± 80.37

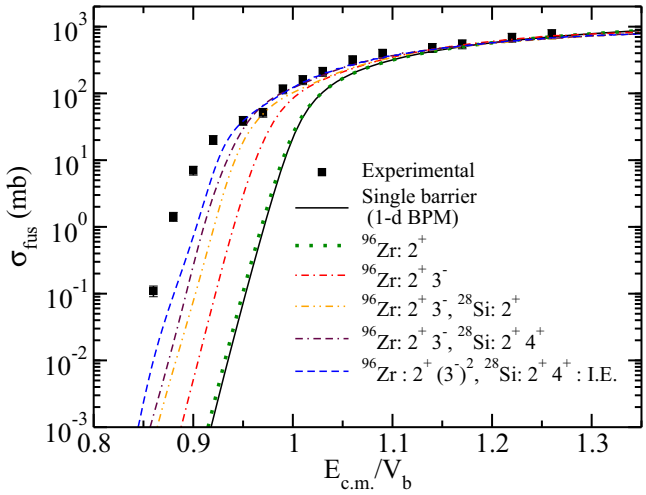

FIG. 3. Experimental fusion excitation function for the ^{28}Si + ^{96}Zr system along with coupled-channels calculations using the CCFULL program. Fusion cross sections with projectile and target inelastic excitations (I.E.) are shown by different curves.

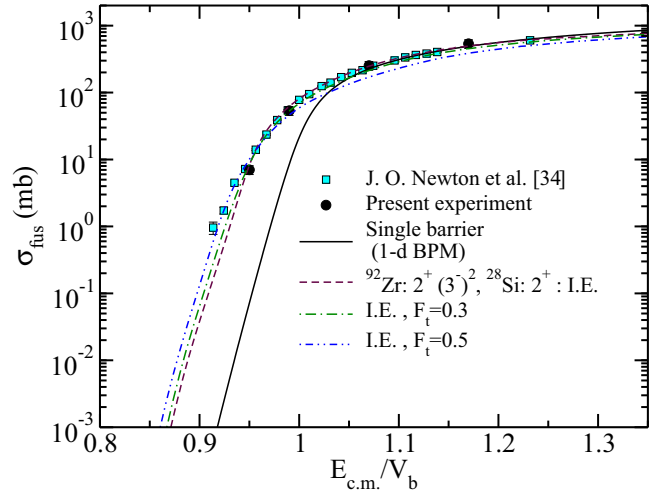

FIG. 5. Experimental fusion excitation function for ^{28}Si + ^{92}Zr along with coupling of the two-neutron transfer channel in addition to inelastic excitations using the CCFULL program.

A. CCFULL

In order to understand the effect of various intrinsic degrees of freedom on fusion, coupled-channels (CC) calculations were performed using the CCFULL program [41]. The fusion excitation function along with CC calculations for ^{28}Si + ^{96}Zr are shown in Figs. 3 and 4. R_b and V_b are the uncoupled single barrier radius and barrier energy respectively, and $E_{c.m.}$ is the center-of-mass energy. The excitation function for the ^{28}Si + ^{92}Zr system is shown in Fig. 5.

To carry out the calculations, Akyuz-Winther (AW) parametrization [42] was employed to obtain Woods-Saxon nuclear potential parameters. The AW potential parameters for ^{28}Si + ^{96,92}Zr along with barrier energy V_b and barrier radius R_b are listed in Table II. Using the AW parameters, fusion cross sections were calculated using the code CCFULL without any couplings. The calculated fusion cross-sections are shown by full lines in Figs. 3–5. It is apparent that the single barrier penetration model (1-d BPM) underpredicts the experimental cross sections. This deviation of 1-d BPM from experimental fusion curve can be resolved with inclusion of low-lying inelastic states and transfer channels. Table III lists the excited states and deformation parameters of projectile as well as target, which can influence the fusion process. The deformation parameter corresponding to multipolarity λ is calculated using adopted values of reduced transition probabilities $B(E\lambda)$ [43,44] except β_4 which is taken directly from Ref. [45]. A value of $r_0 = 1.2$ fm was used to calculate the deformation parameters. Coupled-channels calculations were carried out with ^{28}Si as rotor and ^{96}Zr as a vibrator. Initially, target excitations were incorporated into the calculations. From the 2^+ and 3^- vibrational states of ^{96}Zr, state 3^- seems to be more dominant. After including the 3^- state in CC calculations, cross sections are enhanced by a significant amount whereas the 2^+ state could not give any major contribution to the cross sections. This might be due to the strong octupole deformation strength of ^{96}Zr. This was also observed in an earlier study by Stefanini *et al.* with the ^{36}S + ^{96}Zr system [12]. Projectile excitations were also added successively in the calculations. States 0^+, 2^+, of ^{28}Si give an additional enhancement to the fusion cross sections in the entire energy range. It was observed that the effect of projectile

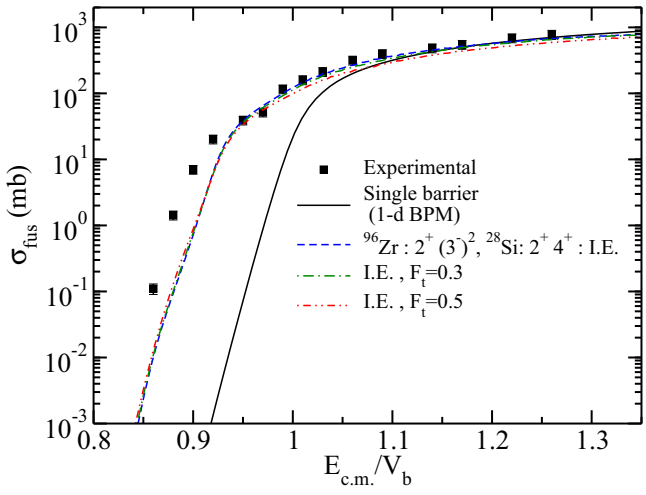

FIG. 4. Experimental fusion excitation function for ^{28}Si + ^{96}Zr along with coupling of the two-neutron transfer channel in addition to inelastic excitations using the CCFULL program.

TABLE II. AW potential parameters (V_0, r_0, a_0) used in theoretical calculations for ^{28}Si + ^{96,92}Zr systems along with barrier energy (V_b) and barrier radius (R_b).

System	V_0 (MeV)	r_0 (fm)	a_0 (fm)	V_b (MeV)	R_b (fm)
^{28}Si + ^{96}Zr	67.82	1.176	0.662	70.87	10.61
^{28}Si + ^{92}Zr	67.25	1.176	0.660	71.58	10.50

TABLE III. Excitation energies E_J and deformation parameters β_J for the excited states, J^π.

Nucleus	J^π	E_J (MeV)	β_J
^{28}Si	2^+	1.78	−0.407
	4^+	4.62	0.250
^{96}Zr	2^+	1.75	0.080
	3^-	1.90	0.283
^{92}Zr	2^+	0.93	0.103
	3^-	2.34	0.174

state 4^+ cannot be neglected for the ^{28}Si + ^{96}Zr system. This 4^+ state of the projectile gives a better fit to above barrier cross sections for ^{96}Zr whereas it overpredicts the cross sections for ^{90}Zr [18]. To obtain a reasonable fit, multiphonon couplings were also included in the CC calculations. ^{28}Si 0^+, 2^+, 4^+ and ^{96}Zr $2^+ \otimes (3^-)^2$ reproduce the experimental data in the high energy region while not explaining the data in below barrier region. Multi-phonon vibrational states such as $(2^+)^2$, $(3^-)^2$, $(2^+)^2 \otimes (3^-)$, $(2^+)^2 \otimes (3^-)^2$, $(2^+) \otimes (3^-)^3$ were also considered in the calculations. These inelastic excitations (I.E.) modified the cross sections slightly, though no combination could simultaneously describe both high and low energy data.

The system ^{28}Si + ^{96}Zr has positive Q value for up to six-neutron transfer channels. Therefore, multineutron transfer channels may be essential for this system and must be included in the coupling scheme to explain the sub-barrier fusion cross sections. Hence, a further step towards the description of low energy data has been taken. The CCFULL program allows us to couple one pair of neutron transfer channels. This program takes into account the transfer channel through a form factor, whose estimation requires study of transfer reactions [46,47]. For the present case, the neutron transfer channel has been added in the coupled-channels calculations through transfer coupling strength parameter (F_t) in the CCFULL program. Coupling strength has been varied in order to get an appropriate fit to experimental fusion cross sections. As can be seen in Fig. 4, the effect of transfer due to $F_t = 0.3$ is indistinct. A slight increase in sub-barrier cross sections due to transfer channel can be observed with $F_t = 0.5$; however, this lowers the above barrier cross sections. It is evident from these calculations that the multineutron transfer may play a crucial role in sub-barrier fusion dynamics, as Q value is positive for up to six-neutron pick-up channels for the system ^{28}Si + ^{96}Zr. The Q values for $1n$ to $6n$ pick-up for the system are 0.62, 4.77, 3.13, 5.60, 1.47, and 1.79 MeV respectively. The effect of transfer has also been examined for ^{92}Zr, where the two-neutron pick-up channel has a positive Q value (3.25 MeV) as shown in Fig. 5. For this system, the coupling strength, $F_t = 0.3$ gives a non-negligible contribution to sub-barrier cross sections, while $F_t = 0.5$ explained the cross sections in the below barrier region though it underpredicted the cross sections in the above-barrier region.

A comparison of reduced fusion excitation functions is shown in Fig. 6 for ^{28}Si + ^{90,92,94,96}Zr to observe the variation in cross sections with increase in the number of positive Q-value transfer channels. A significant amount of enhancement

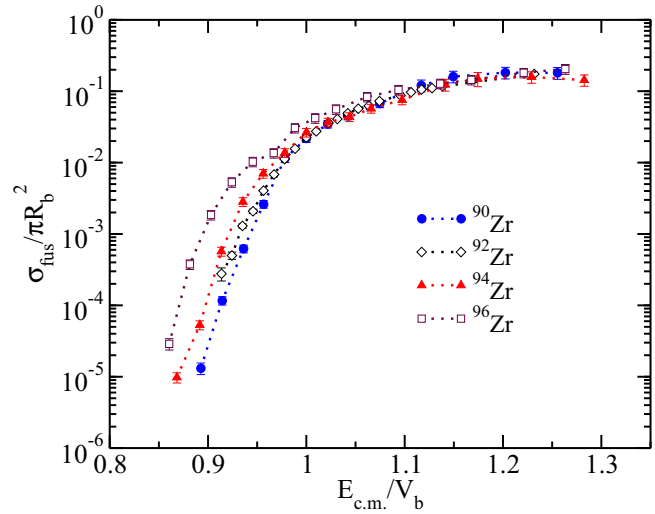

FIG. 6. Fusion excitation function on a reduced scale for ^{28}Si + ^{90,92,94,96}Zr systems (see text). Dotted lines are to guide the eye.

can be seen from ^{90}Zr to ^{96}Zr. The sub-barrier enhancement increases successively with transferred neutrons, which clearly demonstrates the correlation between sub-barrier fusion enhancement and multineutron transfer.

B. Comparison: Si, S, and Ca on ^{96}Zr

In order to examine the role of nuclear structure along with transfer channel on fusion dynamics, a few systems with different structural properties of projectile, for which experimental fusion cross sections are already available, have been compared in Fig. 7. The present analysis was carried out with different projectiles, as presented in Table IV, with ^{96}Zr as the target nucleus for all the projectiles. The experimental

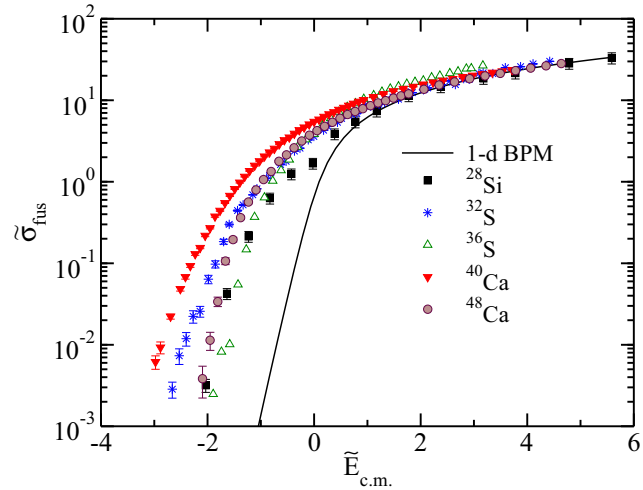

FIG. 7. Comparison of fusion excitation function for various projectiles with ^{96}Zr target on a reduced scale (see text). The experimental fusion cross sections for systems ^{32}S + ^{96}Zr, ^{36}S + ^{96}Zr, ^{40}Ca + ^{96}Zr, and ^{48}Ca + ^{96}Zr have been taken from Refs. [22], [12], [33], and [13] respectively. The fusion cross sections for ^{28}Si + ^{96}Zr are the present experimental data.

TABLE IV. Excitation energies (E_J) and deformation parameters (β_J) for the excited states (J^π) of the selected systems.

Nucleus	J^π	E_J (MeV)	β_J
^{28}Si	2^+	1.78	−0.407
	4^+	4.62	0.250
^{32}S	2^+	2.23	0.320
	3^-	5.01	0.400
^{36}S	2^+	3.29	0.160
	3^-	4.19	-
^{40}Ca	2^+	3.90	0.123
	3^-	3.74	0.330
^{48}Ca	2^+	3.83	0.110
	3^-	4.51	0.250

fusion cross sections for systems ^{32}S + ^{96}Zr, ^{36}S + ^{96}Zr, ^{40}Ca + ^{96}Zr, and ^{48}Ca + ^{96}Zr were taken from Refs. [22], [12], [33], and [13] respectively. The deformation parameters (β_J) along with corresponding excitation energies (E_J) for the low-lying excited states (J^π) of these systems are also listed in the table.

For this systematic study, a procedure was followed for which behavior of 1-d BPM does not depend on the system and can be considered as reference for all the systems [48]. The system independent fusion cross sections and center-of-mass energies have been defined as

$$\widetilde{\sigma}_{\rm fus} = \frac{2\sigma_{\rm fus}E_{\rm c.m.}}{R_{\rm b}^2\hbar\omega}, \quad \widetilde{E}_{\rm c.m.} = \frac{E_{\rm c.m.} - V_{\rm b}}{\hbar\omega},$$

where $\hbar\omega$ is the barrier curvature. Among all the nuclei under consideration, ^{48}Ca and ^{36}S have negative Q values for neutron pick-up channels, hence the transfer channel may not play a major role. However, nucleus ^{40}Ca has positive Q value for the neutron pick-up channel and shows enhancement as expected in the sub-barrier region. In spite of having a large value of the quadrupole deformation parameter (β_2) and the possibility of up to six-neutron pick-up for ^{32}S and ^{28}Si, comparatively less sub-barrier enhancement has been found. To ascertain the effect of transfer channels from the whole sub-barrier fusion enhancement, coupled-channels calculations were carried out using the CCFULL program for the systems ^{28}Si + ^{96}Zr, ^{32}S + ^{96}Zr, and ^{36}S + ^{96}Zr and plotted on a reduced scale, as shown in Fig. 8. The reduction was done using the same expressions of fusion cross section and center-of-mass energy as in case of Fig. 7. The low-lying inelastic states (2^+ and 3^-) of projectile and target were included in the calculations and the effect of these inelastic excitations (I.E.) can be seen in Fig. 8. It was observed that the fusion enhancement could be well explained by including inelastic coupling in the calculations for the system ^{36}S + ^{96}Zr having negative Q value for transfer channels. However, inelastic coupling was unable to reproduce the fusion cross-sections of the other two systems (^{28}Si + ^{96}Zr, ^{32}S + ^{96}Zr) in the sub-barrier region. These systems exhibited almost similar amounts of enhancement after coupling of inelastic excitations, which may be attributed to the presence of positive Q value for up to six-neutron pick-up channels. Apart from these systems, ^{40}Ca + ^{96}Zr also possess positive Q value

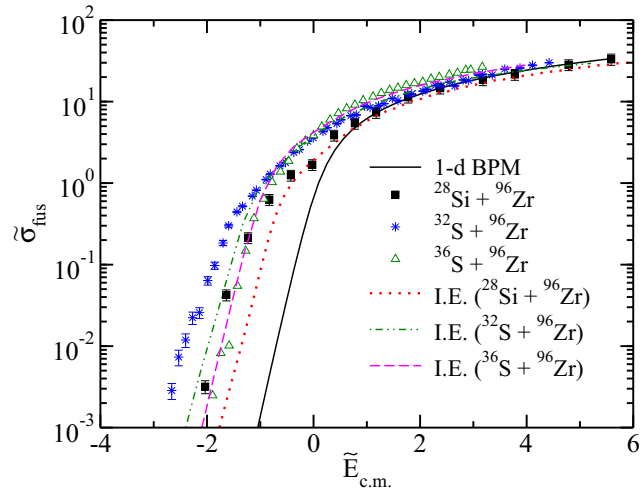

FIG. 8. Experimental fusion cross sections plotted on a reduced scale along with coupled-channels calculations performed with the CCFULL program. The straight lines show the coupling of inelastic excitations (I.E.) of projectile and target states (see text for details).

for multi neutron pick-up channels and has shown the largest enhancement among all the nuclei in Fig. 7. The strong effect of the 3^- state of ^{40}Ca was demonstrated in a recent work [32], which can give a significant contribution to the fusion enhancement due to inelastic excitations in system ^{40}Ca + ^{96}Zr. Besides, the importance of neutron transfer for the large enhancement in ^{40}Ca + ^{96}Zr was demonstrated in [29]. This indicates that inelastic excitations as well as transfer channels play an important role in sub-barrier fusion enhancement; however, influence of the transfer channel can be significant and more clearly visible in a spherical nucleus (^{40}Ca). The fusion enhancement due to transfer channel seems to be less for nuclei having large deformation strength (^{32}S and ^{28}Si).

IV. SUMMARY AND CONCLUSION

This paper presents the fusion excitation function for the systems ^{28}Si + ^{92,96}Zr at energies above and below the Coulomb barrier. Measurements were performed with recoil mass separator HIRA at IUAC. Coupled-channels calculations were performed using the CCFULL program considering the projectile as rotor and the target as a vibrator. Rotational states 2^+ and 4^+ of ^{28}Si and quadrupole excitation along with two-phonon octupole excitation for ^{96}Zr could reproduce the near-barrier data, but are unable to explain the sub-barrier fusion cross sections. The state 3^- of ^{96}Zr was found to be important for explaining the above barrier cross sections. The $2n$ pick-up channel along with inelastic excitations could reproduce the fusion excitation function for ^{92}Zr, whereas multineutron transfer channels appear to be important for ^{96}Zr. A successive increase in sub-barrier fusion cross sections was observed with an increase in the number of neutrons outside the closed shell of Zr.

We presented a comparison between different projectiles, which allowed us to explore nuclear structure effects. Among all the projectiles, ^{40}Ca (doubly magic, $Q > 0$; $+1n$ to $+9n$) showed the highest fusion enhancement, whereas ^{28}Si (oblate shape, $Q > 0$; $+1n$ to $+6n$) showed the lowest enhancement.

The transfer channel seems to be more effective for systems where participating nuclei are spherical or less deformed.

ACKNOWLEDGMENTS

We would like to thank the Pelletron team of IUAC for providing a stable beam throughout the experiment. We are extremely thankful to the target laboratory staff of IUAC, especially Abhilash S. R. for guidance during preparation of the targets. The financial support of the IUAC research Project No. UFR-51314 is gratefully acknowledged. This work has been partly supported by the University of Delhi through a Research and Development grant.

[1] A. B. Balantekin and N. Takigawa, Rev. Mod. Phys. **70**, 77 (1998).
[2] J. R. Leigh, M. Dasgupta, D. J. Hinde, J. C. Mein, C. R. Morton, R. C. Lemmon, J. P. Lestone, J. O. Newton, H. Timmers, J. X. Wei, and N. Rowley, Phys. Rev. C **52**, 3151 (1995).
[3] J. X. Wei, J. R. Leigh, D. J. Hinde, J. O. Newton, R. C. Lemmon, S. Elfstrom, J. X. Chen, and N. Rowley, Phys. Rev. Lett. **67**, 3368 (1991).
[4] C. R. Morton, M. Dasgupta, D. J. Hinde, J. R. Leigh, R. C. Lemmon, J. P. Lestone, J. C. Mein, J. O. Newton, H. Timmers, N. Rowley, and A. T. Kruppa, Phys. Rev. Lett. **72**, 4074 (1994).
[5] A. M. Stefanini, D. Ackermann, L. Corradi, J. H. He, G. Montagnoli, S. Beghini, F. Scarlassara, and G. F. Segato, Phys. Rev. C **52**, R1727 (1995).
[6] A. M. Stefanini, D. Ackermann, L. Corradi, D. R. Napoli, C. Petrache, P. Spolaore, P. Bednarczyk, H. Q. Zhang, S. Beghini, G. Montagnoli, L. Mueller, F. Scarlassara, G. F. Segato, F. Soramel, and N. Rowley, Phys. Rev. Lett. **74**, 864 (1995).
[7] V. Tripathi, L. T. Baby, J. J. Das, P. Sugathan, N. Madhavan, A. K. Sinha, P. V. Madhusudhana Rao, S. K. Hui, R. Singh, and K. Hagino, Phys. Rev. C **65**, 014614 (2001).
[8] L. T. Baby, V. Tripathi, D. O. Kataria, J. J. Das, P. Sugathan, N. Madhavan, A. K. Sinha, M. C. Radhakrishna, N. M. Badiger, N. G. Puttaswamy, A. M. Vinodkumar, and N. V. S. V. Prasad, Phys. Rev. C **56**, 1936 (1997).
[9] A. A. Sonzogni, J. D. Bierman, M. P. Kelly, J. P. Lestone, J. F. Liang, and R. Vandenbosch, Phys. Rev. C **57**, 722 (1998).
[10] R. G. Stokstad, Y. Eisen, S. Kaplanis, D. Pelte, U. Smilansky, and I. Tserruya, Phys. Rev. C **21**, 2427 (1980).
[11] J. D. Bierman, P. Chan, J. F. Liang, M. P. Kelly, A. A. Sonzogni, and R. Vandenbosch, Phys. Rev. Lett. **76**, 1587 (1996).
[12] A. M. Stefanini, L. Corradi, A. M. Vinodkumar, Y. Feng, F. Scarlassara, G. Montagnoli, S. Beghini, and M. Bisogno, Phys. Rev. C **62**, 014601 (2000).
[13] A. M. Stefanini, F. Scarlassara, S. Beghini, G. Montagnoli, R. Silvestri, M. Trotta, B. R. Behera, L. Corradi, E. Fioretto, A. Gadea, Y. W. Wu, S. Szilner, H. Q. Zhang, Z. H. Liu, M. Ruan, F. Yang, and N. Rowley, Phys. Rev. C **73**, 034606 (2006).
[14] H. Esbensen, Phys. Rev. C **72**, 054607 (2005).
[15] A. M. Stefanini, B. R. Behera, S. Beghini, L. Corradi, E. Fioretto, A. Gadea, G. Montagnoli, N. Rowley, F. Scarlassara, S. Szilner, and M. Trotta, Phys. Rev. C. **76**, 014610 (2007).
[16] R. A. Broglia, C. H. Dasso, S. Landowne, and A. Winther, Phys. Rev. C **27**, 2433 (1983).
[17] R. A. Broglia, C. H. Dasso, S. Landowne, and G. Pollarolo, Phys. Lett. B **133**, 34 (1983).
[18] S. Kalkal, S. Mandal, N. Madhavan, E. Prasad, S. Verma, A. Jhingan, R. Sandal, S. Nath, J. Gehlot, B. R. Behera, M. Saxena, S. Goyal, D. Siwal, R. Garg, U. D. Pramanik, S. Kumar, T. Varughese, K. S. Golda, S. Muralithar, A. K. Sinha, and R. Singh, Phys. Rev. C **81**, 044610 (2010).
[19] G. Montagnoli, A. M. Stefanini, H. Esbensen, C. L. Jiang, L. Corradi, S. Courtin, E. Fioretto, A. Goasduff, J. Grebosz, F. Haas, M. Mazzocco, C. Michelagnoli, T. Mijatovic, D. Montanari, C. Parascandolo, K. E. Rehm, F. Scarlassara, S. Szilner, X. D. Tang, and C. A. Ur, Phys. Rev. C **87**, 014611 (2013).
[20] M. Trotta, A. M. Stefanini, L. Corradi, A. Gadea, F. Scarlassara, S. Beghini, and G. Montagnoli, Phys. Rev. C **65**, 011601(R) (2001).
[21] G. Montagnoli, A. M. Stefanini, C. L. Jiang, H. Esbensen, L. Corradi, S. Courtin, E. Fioretto, A. Goasduff, F. Haas, A. F. Kifle, C. Michelagnoli, D. Montanari, T. Mijatovic, K. E. Rehm, R. Silvestri, P. P. Singh, F. Scarlassara, S. Szilner, X. D. Tang, and C. A. Ur, Phys. Rev. C **85**, 024607 (2012).
[22] H. Q. Zhang, C. J. Lin, F. Yang, H. M. Jia, X. X. Xu, Z. D. Wu, F. Jia, S. T. Zhang, Z. H. Liu, A. Richard, and C. Beck, Phys. Rev. C **82**, 054609 (2010).
[23] A. M. Stefanini, G. Montagnoli, F. Scarlassara, C. L. Jiang, H. Esbensen, E. Fioretto, L. Corradi, B. B. Back, C. M. Deibel, B. Di Giovine, J. P. Greene, H. D. Hendersen, S. T. Marley, M. Notani, N. Patel, K. E. Rehm, D. Sewerinyak, X. D. Tang, C. Ugalde, and S. Zhu, Eur. Phys. J. A **49**, 63 (2013).
[24] Z. Kohley, J. F. Liang, D. Shapira, R. L. Varner, C. J. Gross, J. M. Allmond, A. L. Caraley, E. A. Coello, F. Favela, K. Lagergren, and P. E. Mueller, Phys. Rev. Lett. **107**, 202701 (2011).
[25] H. M. Jia, C. J. Lin, F. Yang, X. X. Xu, H. Q. Zhang, Z. H. Liu, L. Yang, S. T. Zhang, P. F. Bao, and L. J. Sun, Phys. Rev. C **86**, 044621 (2012).
[26] V. V. Sargsyan, G. G. Adamian, N. V. Antonenko, W. Scheid, and H. Q. Zhang, Phys. Rev. C **84**, 064614 (2011).
[27] G. L. Zhang, X. X. Liu, and C. J. Lin, Phys. Rev. C **89**, 054602 (2014).
[28] A. A. Ogloblin, H. Q. Zhang, C. J. Lin, H. M. Jia, S. V. Khlebnikov, E. A. Kuzmin, W. H. Trzaska, X. X. Xu, F. Yan, V. V. Sargsyan, G. G. Adamian, N. V. Antonenko, and W. Scheid, Eur. Phys. J. A **50**, 157 (2014).
[29] V. A. Rachkov, A. V. Karpov, A. S. Denikin, and V. I. Zagrebaev, Phys. Rev. C **90**, 014614 (2014).
[30] D. Bourgin, S. Courtin, F. Haas, A. M. Stefanini, G. Montagnoli, A. Goasduff, D. Montanari, L. Corradi, E. Fioretto, J. Huiming, F. Scarlassara, N. Rowley, S. Szilner, and T. Mijatovic, Phys. Rev. C **90**, 044610 (2014).
[31] A. M. Stefanini, G. Montagnoli, L. Corradi, S. Courtin, D. Bourgin, E. Fioretto, A. Goasduff, J. Grebosz, F. Haas, M. Mazzocco, T. Mijatovic, D. Montanari, M. Pagliaroli, C. Parascandolo, F. Scarlassara, E. Strano, S. Szilner, N. Toniolo, and D. Torresi, Phys. Rev. C **92**, 064607 (2015).

[32] J. F. Liang, J. M. Allmond, C. J. Gross, P. E. Mueller, D. Shapira, R. L. Varner, M. Dasgupta, D. J. Hinde, C. Simenel, E. Williams, K. Vo-Phuoc, M. L. Brown, I. P. Carter, M. Evers, D. H. Luong, T. Ebadi, and A. Wakhle, Phys. Rev. C **94**, 024616 (2016).

[33] H. Timmers, D. Ackermann, S. Beghini, L. Corradi, J. He, G. Montagnoli, F. Scarlassara, A. M. Stefanini, and N. Rowley, Nucl. Phys. A **633**, 421 (1998).

[34] J. O. Newton, C. R. Morton, M. Dasgupta, J. R. Leigh, J. C. Mein, D. J. Hinde, H. Timmers, and K. Hagino, Phys. Rev. C **64**, 064608 (2001).

[35] Khushboo, Abhilash S. R., D. Kabiraj, and S. Mandal, Proc. DAE Symp. Nucl. Phys. **59**, 964 (2014).

[36] Khushboo, Abhilash S. R., D. Kabiraj, S. Ojha, and S. Mandal, Proc. DAE-BRNS Symp. Nucl. Phys. **60**, 1036 (2015).

[37] R. Bass, *Nuclear Reactions with Heavy Ions* (Springer-Verlag, Berlin, 1980).

[38] A. K. Sinha, N. Madhavan, J. J. Das, P. Sugathan, D. O. Kataria, A. P. Patro, and G. K. Mehta, Nucl. Instrum. Methods Phys. Res., Sect. A **339**, 543 (1994).

[39] E. T. Subramaniam, B. P. Ajith Kumar, and R. K. Bhowmik, software CANDLE: Collection and Analysis of Nuclear Data using Linux nEtwork (unpublished).

[40] S. Nath, Comput. Phys. Commun. **180**, 2392 (2009).

[41] K. Hagino, N. Rowley, and A. T. Kruppa, Comput. Phys. Commun. **123**, 143 (1999).

[42] R. A. Broglia and A. Winther, *Heavy Ion Reaction Lecture Notes, Vol. 1: Elastic and Inelastic Reactions* (Benjamin Cummings, Reading, MA, 1981).

[43] S. Raman, C. W. Nestor, Jr., and P. Tikkanen, At. Data Nucl. Data Tables **78**, 1 (2001).

[44] T. Kibedi and R. H. Spear, At. Data Nucl. Data Tables **80**, 35 (2001).

[45] P. Moller, J. R. Nix, W. D. Myers, and W. J. Swiatecki, At. Data Nucl. Data Tables **59**, 185 (1995).

[46] C. H. Dasso and G. Pollarolo, Phys. Lett. B **155**, 223 (1985).

[47] S. Saha, Y. K. Agarwal, and C. V. K. Baba, Phys. Rev. C **49**, 2578 (1994).

[48] N. V. S. V. Prasad, A. M. Vinodkumar, A. K. Sinha, K. M. Varier, D. L. Sastry, N. Madhavan, P. Sugathan, D. O. Kataria, and J. J. Das, Nucl. Phys. A **603**, 176 (1996).